

# Performance of Concrete Tunnel Systems Subject To Fault Displacement

Ashutosh Garg (M.Tech Scholar)  
Mr Murlī Chourasiya (Guide)  
Mr. Rahul Satbhāiya ( HoD )  
Infinity Engineering and Management College  
Sagar (M.P.)

**Abstract:** A Finite Element Analysis (FEA) investigation of concrete tunnel systems traversing seismic faults is carried out to determine how to effectively mitigate the stresses induced in the liner when subject to fault displacement. A parametric study of various fault parameters, both in the damage zone and competent rock, is carried out to determine the site conditions which induce the most stress on the tunnel liner system. Results indicate that friction angle, cohesion, and elastic modulus of fault zones have varying effects on the stresses induced on the liner. The width of damage zone and expected displacements are also investigated and it has been shown that even small displacements over narrow damage zones, around 10 m, can still result in significant damage to the concrete liner whereas in wider damage zones the effects of the displacement are more evident. The use of flexible joints in what is known as the articulated design method is investigated to mitigate the stresses induced by fault displacement and discussed. Several orientations, lengths and variations in relative stiffness of these flexible joints are investigated to determine their optimal effectiveness. Results show that this is an effective solution which can be used in design and repair of tunnels to mitigate the stresses and resulting damages to concrete tunnel liners subject to fault displacement.

Date of Submission: 04-01-2022

Date of acceptance: 15-01-2022

## I. INTRODUCTION

Tunneling is a large industry, from the underground construction of transportation tunnels to relieve surface congestion to lifeline systems required to provide essential utilities. Although avoided if possible, it becomes inevitable that some of these systems will cross faults in seismically active regions. This is a problem in areas such as the state of California which is a well-documented, seismically active area, namely due to the San Andreas Fault system in southern California. Tunnels in these regions are not only subject to dynamic loading from earthquakes, but those which cross active faults are also subject to a large degree of fault dislocation. Stability, strength and serviceability immediately become issues as the tunnel is forced to deform with the fault, which can cause major damage to the concrete tunnel liner. Figure 1.1 illustrates the damage to tunnel liners due to the shear deformations imposed by the surrounding ground. The mitigation of damage to tunnel liners caused by fault dislocation is the focus of this research.

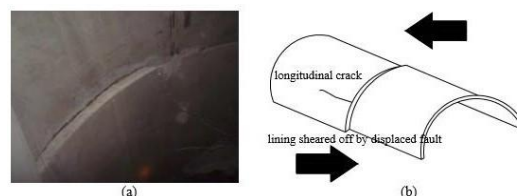


**Figure 1:** Sheared off lining due to displaced fault.

## II. TUNNELS & BACKGROUND OF TUNNELING

Tunnels are constructed in a multitude of ground conditions varying from soft clays to hard rocks and the method of construction is highly dependent on these ground conditions as well as other factors, such as groundwater conditions, depth of tunnel and diameter of the tunnel. Today, there are three general methods of tunnel construction: cut- and-cover tunneling, immersed tunneling, and bored tunneling as depicted by Figure 1.2. In this research the latter method is of most concern as cut-and-cover and immersed tunnels are not subject to fault displacement to the same degree as bored tunnels. The methods of tunneling described herein, are not meant to be an exhaustive detailing or design procedure of each method, but rather a succinct description of the

approach and evolution of each method. It should be noted the methods described here are not the only methods of tunnel construction used in practice.

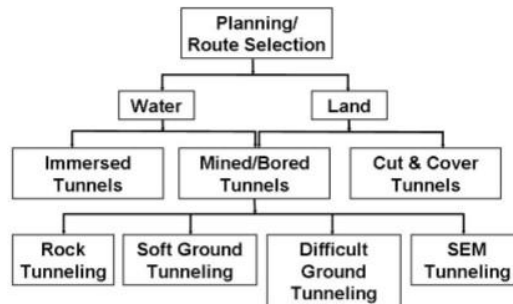


Figure 2: Preliminary tunnel type selection for a typical road tunnel

### III. LITERATURE REVIEW

This section will describe several aspects and methods of modeling faults, soil and rock properties for the purposes of accurately capturing tunnel-fault interaction necessary to develop the parametric relationships required for this research. This section is primarily organized from the simpler modeling of soil behavior to more detailed methods of modeling. This is specifically done to highlight the complexities and intricacies of soil behavior and to reinforce the difficulties in accurately modeling this behavior. In fact, Ladd et al. (1977) summarizes this point quite well,

“The ideal soil behavior model would describe the soil’s deformation and pore pressure response under all types of loading conditions at any time, strength being incorporated as an upper limit to the stress-strain relationship ... A generalized model of the stress-strain behavior of soils should ideally account for nonlinearity, yielding, variable dilatancy (volume changed cause by shear stress), and anisotropy (both inherent and stress system induced), plus the behavioral dependence on stress path, stress system (orientation of  $\sigma_1$  and relative magnitude of  $\sigma_2$ ), and stress history (both initial and changes due to consolidation).” – pg. 454

Russo et al. (2002) discusses fault crossing strategies for twin shield tunnels (specifically for the Bolu Tunnel project) crossing the Bakacak Fault and the Zekidaği Fault in Turkey. In 1999, after the Düzce earthquake (MW = 7.2), a detailed seismic reconnaissance of the area around the Bolu Tunnel project was carried out, allowing for a more accurate modeling of the two faults for the study. The Zekidaği Fault dips approximately 90 degrees with the tunnel crossing this fault over the length of 25 to 30 m (82 to 98 ft.) in both tubes. This fault was identified with low potential for future rupture with an estimated right lateral offset displacement of 0.15 to 0.25 m (5.91 to 9.84 in) from an associated earthquake with magnitude MW from 6 to 6.25. The Bakacak Fault dips approximately 40 degrees with the tunnel crossing this fault over the length of 100 m (328 ft). Estimated rupture displacements are up to 0.5 m (19.69 in) from an associated earthquake with magnitude MW from 6.25 to 6.5. Fault ruptures may occur in a concentrated or a distributed manner, and for the Bakacak Fault it was assumed – then justified by geologists, that its displacements would most likely be distributed and mainly horizontal whereas the displacements at the Zekidaği Fault could not be accurately predicted. Because of this previous assumption, the researchers were able to assume the shear strain in the fault soil as the ratio between expected offset and width of the fault at tunnel level. The soil was modeled as Mohr- Coulomb (M-C) compression springs using contact elements between the tunnel liner and soil.

Daller & Weigl (2011) investigated concepts for the new Semmering Base Tunnel in Austria to find a support and construction process which would provide tunnel displacements compatible with the fault system using FLAC2D. This tunnel was constructed through the Graßberg-Schlagl fault system and rock characteristics for this system were determined by triaxial compression tests from core samples. The results from a triaxial compression test on one specimen was back-calculated using the finite element program ZSoil, considering the Hardening Soil (HS) – Small Strain constitutive law as well as the M-C constitutive law to help determine the relevancy of a nonlinear analysis. Obrzud (2010) discusses the significance of using the HS model as opposed to the M-C model in ZSoil and ultimately concluded that the HS model is the more accurate model to use in finite element analysis. The linear-elastic M-C model does not always give reliable and realistic predictions in FEA because soil is only truly elastic at very small strains. The HS- Standard Model considers the pre-failure nonlinearities of soil behavior while reproducing basic macroscopic phenomena exhibited by soils such as densification, stress dependent stiffness, soil stress history, plastic yielding and dilatancy (Obrzud 2010). Moreover, the advanced version of this model, the HS-Small Strain model, incorporates the above phenomena along with strong stiffness variation as well as the hysteretic, nonlinear elastic stress-strain relationship of a soil (Obrzud 2010). Obrzud (2010) reanalyzed the tunnel excavation of the twin Jubilee Line Extension Project in London, UK using HS models as well as the M-C model to prove that the HS models give more realistic stress-

strain behavior of the soil by comparing results to triaxial lab tests shows that at very small strains ( $< 0.01\%$  axial strain) the HS-Small and M-C Models accurately model the behavior captured during isotropically consolidated undrained extension (CIUE) tests. However, it can be seen that at larger strains, the HS-Model is what actually captures the soil's behavior across the range of strains expected. In fact, the HS- Small model used by Daller & Weigl (2011) also agreed well with lab data constructed from triaxial compression tests compared to the M-C model which did not accurately fit to the data.

Wang et al. (2012) used FLAC3D to model tunnels crossing active faults subjected to a differential displacement across the fault. A fault zone, as opposed to a discrete fault plane, was modeled and the fault displacement was estimated to be 0.2 m. However, the width of the modeled fault zone was not specified, although a finite thickness can be assumed from Figure 2.4, which shows a profile of their tunnel-fault model in FLAC3D. The tunnel liner is modeled using three dimensional elastic elements and ground behavior was modeled using the M-C criterion. Wang et al. (2012) found that under strike-slip conditions, the damage to surrounding rock and tunnel liner were more serious than that of the other fault conditions analyzed, as per Figure 2.5, thus their flexible joint design is based on strike-slip conditions.

#### IV. FINITE ELEMENT MODELING

This section describes the methods of modeling the tunnel and surrounding ground for preliminary elastic analysis as well as nonlinear analysis. Geometries (tunnel and ground), meshing, boundary conditions and mechanical properties are all outlined in this chapter.

Concrete behavior of the tunnel liner is represented using the Hognestad (1951) material model of unconfined concrete to account for the nonlinearity in the stress-strain behavior of concrete. Equations are included to also modify the behavior of plain concrete to represent the behavior of fiber-reinforced concrete. Effort is also made to account for the nonlinear, anisotropic, stress-dependent behavior of soil and rock included in this modeling.

##### I) Geometry

The three-dimensional geometries for tunnels, fault zone and surrounding ground were created using SpaceClaim3D design modeling software built into the ANSYS Workbench program. Using this software allowed for easy integration into the ANSYS program for finite element analysis.

In preliminary analysis, the foot wall and hanging wall of the fault are identically sized rectangular prisms (100 m x 50 m x 100 m) placed together to result in a fault zone modeled by 3D solid elements. The two walls of the fault meet at the fault plane with a dip of  $90^\circ$ , and this plane is where the entirety of the fault dislocation occurs. Figure 3.1 shows profile and cross-sectional views of the ground geometry surrounding the assumed fault. This geometry was created for the sole purpose of preliminary, linear analysis to determine how to apply displacements and check if the distribution of stresses throughout the model made sense before moving onto nonlinear analysis. There are also models created where distributed displacements will be applied. This is done by including a third rectangular prism in between the two walls of the fault, the damage zone, where distributed displacements across the width of the damage zone will be applied. Per pertinent literature discussed in Section 2.2, three additional geometries were created with damage zones of 10 m, 50 m, and 100 m (32 ft, 164 ft, and 328 ft) which can be seen in Figure 3.2. In these models, widths of the footwall and hanging wall are held constant at 50 m (164 ft). The reason that the widths of the competent rock (footwall and hanging wall) are held constant is because results from preliminary analysis show there is no significant boundary influence on stresses using widths of 50 m from where the fault displacement is applied.

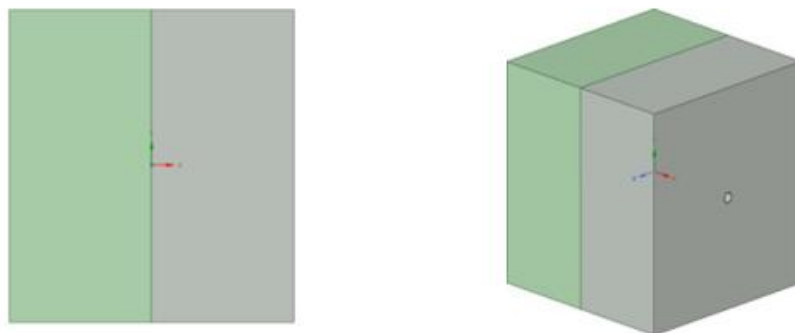


Figure 3: a) plan view of ground and fault geometry where the green highlighted body is the footwall and the light gray body is the hanging wall of the FEM. b) shows location of tunnel in elevation, passing through the fault.

## II) Meshing

An effective mesh is important in this analysis to provide accurate results without becoming too computationally expensive. The Automatic Meshing feature within ANSYS resulted in an effective mesh meeting these criteria. The mesh used is a rectangular mesh for both the tunnel and ground with a mesh refinement value of 1 over the entire model. The rectangular meshed elements appear regular away from the tunnel and begin to change shape into irregular, angular shapes which decrease in size closer to the modeled tunnel. Figure show the meshing of the ground and tunnel, respectively. During nonlinear analysis, the mesh will be refined in the area immediately surrounding the fault zone to gain more accurately capture the behavior of the tunnel liner subjected to fault displacement.

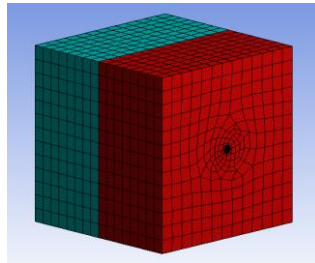


Figure 4: Automatic meshing of the ground surrounding the tunnel. The light blue body is the footwall and the red body indicates the hanging wall.

## III) Boundary Conditions & Contact Interfaces

To capture the effects due to fault dislocation in the immediate area of the fault, proper modeling of boundary conditions is essential. The plane of the foot wall opposite to the fault plane is fixed in space while the plane of the hanging wall opposite of the fault plane is modeled as a frictionless (roller) support, which allows the hanging wall to move freely in the y and z degrees of freedom. In preliminary analyses the effect of the proximity of the boundary condition on the behavior of the tunnel at the fault plane was studied and determined that 50 m (164 ft) is enough to negate any boundary effects on the stress induced by faulting.

## V. Analysis Options & Fault Displacement

The Static Structural analysis type as defined in ANSYS Workbench is run for this research. For this type of analysis, the direct solver option is more often used than the iterative solver for the sake of decreasing the computational expenses, although both solvers result in equal results.

In the preliminary analysis to determine stress distributions in the liner, to simulate the active faulting, a 0.05 m displacement is applied to the face of the hanging wall at the frictionless boundary with the foot wall. Again, this displacement of 0.05 m is arbitrary just to look at basic effects of faulting in preliminary modeling and trials. The applied displacements at the fault are applied parallel to the fault plane and can be applied in any direction, but in the case of this research are applied in the global y-axis direction. Because the preliminary modeling was linear and displacement relative to the size of the tunnel and overall model is small, the displacement is being run over only one time-step with program- controlled auto time stepping.

After preliminary analysis, the next stage of analysis begins with applying a distributed 1 m displacement over the damage zone of the model for each damage zone width (10 m, 50 m, 100 m). This displacement was purposefully chosen as a reasonable fault displacement which can be encountered from an earthquake. This displacement is applied over four manually created time-steps. In this stage of analysis, where nonlinear concrete properties were also included to mimic the Hognestad parabola, it was determined that auto time stepping, which allows ANSYS WB to automatically create sub-steps to capture nonlinearity in models, is adequate to capture the nonlinear behavior of the concrete without having to manually create many sub-steps. The proof of this can be seen in Figure 3.17, which shows the auto time stepping correctly capturing the nonlinear behavior as well as a model which was forced to have 20 sub-steps per time step. The main advantage of allowing ANSYS WB to automatically create sub-steps is that computational time is drastically decreased from when manual sub-steps are created.

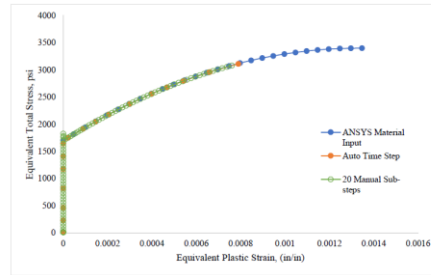


Figure 5: Plot of equivalent total stress versus plastic strain of concrete element including the nonlinear concrete input to show nonlinearity is captured sufficiently using automatic time stepping.

V. RESULTS

Models run in this section show that the competent rock behaves linearly with the applied displacement of 1 m and although the stresses in the rock may change when nonlinear controls are turned on, the stresses induced in the nonlinear tunnel liner remain the same. The lowest reasonable value for elastic modulus in competent rock is about 2,000 MPa and for the damage zone the lowest reasonable value is about 50 MPa. Using a 10 m damage zone model where the elastic modulus of the damage zone and competent rock as described above along with 0.2 value for Poisson’s Ratio was applied. From pertinent literature discussed in Sections 2.4 and 3.5, the lowest reasonable cohesion value for competent rocks is about 6.7 MPa which was also applied to the competent rock in the models. The initial inner friction angle in the competent rock and damage zone were set to 40° and 30°, respectively, typical values from literature. The ratios for residual friction angle and dilatancy angle to initial inner friction angle are set at 0.5 and 1.0 for both rocks. The range of cohesion values in damage zone rock ranges from 0.1 MPa up to 1.0 MPa and are also tested to prove linearity in competent rock. The ratio of residual cohesion to initial cohesion is 1.0 for both rocks as well. Table 4.1 presents the properties of the two models, NL1-1 and NL1-2, just described.

Table 1: Table of rock properties used for models NL1-1 and NL1-2.

Competent Rock Properties						
	Initial Inner Friction Angle, $\phi$ (°)	Residual Inner Friction Angle, $\phi_r$ (°)	Dilatancy Angle, $\psi$ (°)	Initial Cohesion, c (MPa)	Residual Cohesion, cr (MPa)	Elastic Modulus, E (MPa)
NL 1-1	40	20	40	6.7	6.7	2,000
NL 1-2	40	20	40	6.7	6.7	2,000
Damage Zone Properties						
	Initial Inner Friction Angle, $\phi$ (°)	Residual Inner Friction Angle, $\phi_r$ (°)	Dilatancy Angle, $\psi$ (°)	Initial Cohesion, c (MPa)	Residual Cohesion, cr (MPa)	Elastic Modulus, E (MPa)
NL 1-1	30	15	30	0.5	0.5	50
NL 1-2	30	15	30	0.5	0.5	50

To determine if the value of initial cohesion defined in the competent rock affects the model results, cohesion was increased to 10 MPa in model NL1-3 to see if results change. Figures 4.19-4.22 show that increasing the cohesion did not affect the stresses induced in the tunnel liner which indicates that the cohesion is high enough in the competent rock such that the rock will always behave linearly, within the range of reasonable values of cohesion tested. The properties of the models in these figures are presented in Table 4.2. The initial inner friction angle is changed to a low, reasonable value for intact rock, 15° in model NL1-5. The results from changing the initial inner friction angle from to a low value and comparing it to a model where the initial inner friction angle of the competent rock is at a high value, 50° in model NL1-4. These figures show the lines plot on top of one another, further proving that nonlinearity in the competent, intact rock is controlled by the value of initial cohesion, and since it is proven that the minimum value used does not invoke nonlinearity in the models even when the initial inner friction angle is varied, the competent rock can be run linearly.

Table 2: Table of rock properties used for models NL1-2 and NL1-3.

Competent Rock Properties						
	Initial Inner Friction Angle, $\phi$ (°)	Residual Inner Friction Angle, $\phi_r$ (°)	Dilatancy Angle, $\psi$ (°)	Initial Cohesion, c (MPa)	Residual Cohesion, cr (MPa)	Elastic Modulus, E (MPa)
NL 1-2	40	20	40	6.7	6.7	2,000
NL 1-3	40	20	40	10	10	2,000

	Damage Zone Properties					
	Initial Inner Friction Angle, $\phi$ (°)	Residual Inner Friction Angle, $\phi_r$ (°)	Dilatancy Angle, $\psi$ (°)	Initial Cohesion, $c$ (MPa)	Residual Cohesion, $c_r$ (MPa)	Elastic Modulus, $E$ (MPa)
NL 1-2	30	15	30	0.5	0.5	50
NL 1-3	30	15	30	0.5	0.5	50

## VI. CONCLUSION

In this paper a FEA investigation of tunnels traversing seismic fault zones is reported. Parameters of competent rock and damage zone rock properties were studied to observe their effects on tunnel liner damage. The use of articulated tunnel liners to mitigate liner damage was also evaluated. A literature review was completed to determine appropriate ranges of material properties and fault displacements.

Results show that competent rock can be modeled as linear-elastic using only the elastic properties for up to 1.0 m fault displacement investigated, and for the properties gained from literature review. It was also determined the M-C properties of the damage zones have effects of varying degrees. In 10 m damage zones subject to 1 m of fault displacement, surrounded by softer competent rock ( $E = 2,000$  MPa), the effects of the cohesion and friction angle of the faulted rock are evident in the stress distribution of the tunnel liner outside of the damage zone into the competent rock though full yielding of the liner in the damage zone was observed for all cases. Higher friction angle and lower cohesion result in the highest stress values in the competent rock section of the tunnel. These stresses do not have a critical enough impact such that special care and design be undertaken to mitigate these stresses. However, in cases where the faulted rock is surrounded by stiffer competent rock ( $E = 100,000$  MPa), it is the elastic properties of the competent rock that control the stress distributions in the tunnel liner outside of the damage zone instead of the M-C properties of the faulted rock in the damage zone. So, it is recommended that special care be taken to accurately measure the M-C properties in short damage zones surrounded by soft rock so that they can be accurately modeled to determine stress distributions throughout the tunnel liner, however this is not as critical in damage zones surrounded by hard rock. But in hard rock, special care should be taken in measuring the elastic properties, so it can be determined if the stresses into the competent rock are critical enough for the given design such that they can be designed for expected fault displacement.

In long damage zones, around 50 m in length and greater, lower cohesion and higher friction angles of the damage zone rock create slightly higher stress values in the portion of the tunnel liner crossing the damage zone. However, these M-C properties are less critical than in the shorter damage zone of 10 m investigated. The portion of the tunnel liner outside the damage zone, in the competent rock, the stress distributions are controlled by the elastic properties of the competent rock. In damage zones of these lengths and greater it is likely that the elastic properties of the rock are what dominate the stresses induced in the tunnel liner outside of the damage zone. It seems that as the damage zone increases in length, the M-C properties of the damage zone become less important in determining the stress distribution in the tunnel liner. Models with elastic moduli of the damage zone greater than 50 MPa can only undergo a fraction of the displacement that it can in softer ground. Special care should be taken in stiffer damage zones to evaluate stress distributions in the tunnel liner caused by fault displacements as they could only withstand smaller fault displacements in the FEA. Investigating the use of the over-excavation method as a possible solution to allow these tunnels to move through expected fault displacements is suggested.

The results of this research can be used to focus a design approach when specific information about fault width, expected dislocation and ground properties are known. Details of links in an articulated design could be engineered to match the moment curvature relationships assumed in these models.

## REFERENCES

- [1]. Bickel, J. O., Kuesel, T. R., & King, E. H. (1996). *Tunnel Engineering Handbook*. Boston, MA: Springer US.
- [2]. C. Ladd, C & Foott, R & Ishihara, K & Schlosser, F & Poulos, Harry. (1977). *Stress – deformation and strength characteristics: state of the art report*. Proc. 9th Int. Conf. Soil Mechs. Foundn. Engng., Tokyo. 2.
- [3]. Cochran, Elizabeth & Li, Yong-Gang & M. Shearer, Peter & Barbot, Sylvain & Fialko, Yuri & Vidale, John. (2009). *Seismic and geodetic evidence for extensive, long lived fault damage zones*. *Geology*. 37. 315-318. 10.1130/G25306A.1.
- [4]. Daller, Josef & Weigl, Johannes. (2011). *The new Semmering base tunnel – tunnel design in the fault zone / Semmering-Basistunnel neu – Tunneldesign in der Störungszone*. *Geomechanics and Tunneling*. 4. 10.1002/geot.201100015.
- [5]. Davis, G. H., Reynolds, S. J., & Kluth, C. (2012). *Structural geology of rocks and regions*.
- [6]. Ding, Jun-Hong & Xianlong, Jin & Guo, Yi-Zhi & Li, Gen-Guo. (2006). *Numerical simulation for large-scale seismic response analysis of immersed tunnel*. *Engineering Structures*. 28. 1367-1377. 10.1016/j.engstruct.2006.01.005.
- [7]. Earle, S. (2015). *Physical geology*.
- [8]. F. Obrzud, Rafał. (2018). *On the use of the Hardening Soil Small Strain model in geotechnical practice*.
- [9]. H. Kulhawy, Fred. (1975). *Stress deformation properties of rock and rock discontinuities*. *Engineering Geology*. 9. 327-350.
- [10]. Karakus, Murat & Fowell, R. (2004). *An insight into the New Austrian Tunneling Method (NATM)*. ROCKMEC'2004-VIIth Regional Rock Mechanics Symposium, 2004, Sivas, Türkiye.

- [11]. Lee, Seong-Cheol & Oh, Joung-Hwan & Cho, Jae-Yeol. (2015). *Compressive Behavior of Fiber-Reinforced Concrete with End-Hooked Steel Fibers*. Materials. 8. 1442-1458. 10.3390/ma8041442.
- [12]. Łotysz, Sławomir. (2010). *Immersed tunnel technology: A brief history of its development*. Civil and Environmental Engineering Reports. 97-110.
- [13]. Luo, X., Yang, Z. 2013. *Finite element modeling of a tunnel affected by dislocation of faults*. APCOM & ISCM. Singapore, December 11-14.
- [14]. M. Savage, Heather & Brodsky, Emily. (2011). *Collateral damage: Evolution with displacement of fracture distribution and secondary fault strands in fault damage zones*. Journal of Geophysical Research. 116. 10.1029/2010JB007665.
- [15]. Mohammed, Jaafar. (2014). *Textbook: Engineering Geology & Tunnels Engineering*. 10.13140/RG.2.2.21898.06084.
- [16]. Ohbo, Naoto, Furuya, Takashi, Takamatsu, Ken, Komaki, Shouzou. (2000). *Seismic Behavior of Shield Tunnel Across Active Fault*. Annual Report, Kajima Technical Research Institute, Kajima Corporation. 48. 165-166. ISSN 0918015X.
- [17]. Roach, Michael F., Colin A. Lawrence, and David R. Klug. (2017). *The history of tunneling in the United States*.
- [18]. Russo, M., Germani, G., & Amberg, W. (2002). *Design and construction of large tunnel through active faults: A recent application*. In International conference of tunneling & underground space use, Istanbul, Turkey, 16–18 October.
- [19]. Shahidi, Alireza & Vafaeian, Mahmood. (2005). *Analysis of longitudinal profile of the tunnels in the active faulted zone and designing the flexible lining (for Koohrang III tunnel)*. Tunnelling and Underground Space Technology. 20. 213-221.
- [20]. T.M. Mitchell, D.R. Faulkner. (2009). *The nature and origin of off-fault damage surrounding strike-slip fault zones with a wide range of displacements: A field study from the Atacama fault system, northern Chile* Journal of Structural Geology. Volume 31. Pages 802-816.
- [21]. T.M. Mitchell, Y. Ben-Zion, T. Shimamoto. (2011). *Pulverized fault rocks and damage asymmetry along the Arima-Takatsuki Tectonic Line, Japan*. Earth and Planetary Science Letters, Volume 308, Issues 3–4, 2011, Pages 284-297, ISSN 0012-821X. Volume 31, Issue 8, 2009, Pages 802-816, ISSN 0191-8141.